Prediction of Post-Cracking Behaviour in SFRC Elements Under in-Plane Stresses

P. Bernardi[1], R. Cerioni[1] and E. Michelini[1]

[1] Dept. of Civil and Environmental Engineering and Architecture, University of Parma viale G.P. Usberti 181/A – 43124 Parma (Italy),
patrizia.bernardi@unipr.it, roberto.cerioni@unipr.it, elena.michelini@unipr.it

ABSTRACT. *In recent years, the use of steel fibre reinforced concrete (SFRC) has increasingly spread in several engineering fields. However, the use of this composite material requires an adjustment of the computational tools normally adopted in current design, as well as a review of the implemented constitutive relationships, which are usually referred to ordinary plain or reinforced concrete. In this paper, this problem has been tackled by means of a numerical procedure, based on nonlinear fracture mechanics concepts, which allows to correctly simulate the fibre contribution, especially in the post-cracking stage. More in detail, a macroscopic model (named 2D-PARC), already developed for ordinary RC structures, has been extended to SFRC elements subjected to plane stresses, by taking into account realistic semi-empirical constitutive laws for concrete, steel fibres and ordinary reinforcement. The effectiveness of the proposed approach has been verified through comparisons with significant experimental full-scale tests available in technical literature concerning SFRC beams, with or without traditional reinforcement.*

INTRODUCTION

The increasing use of steel fibres in partial or total substitution of conventional reinforcement is mainly related to the improvement in concrete performances [1-3] and to the significant labour saving in construction phases, which make this solution particularly attractive for different structural applications.

While in the past the use of SFRC was mainly limited to those structural applications for which the use of fibres was not essential for safety issues (such as industrial pavements), more recently an increasingly interest has grown in their use for structural members subjected to bending and shear, like beams. On this point, several experimental studies carried out on RC beams with and without stirrups ([4-8] among others) have demonstrated that the global behaviour of these elements can be significantly enhanced, both in terms of strength and ductility, by adding steel fibres to the concrete mix, with an optimum percentage between 0.5 and 1.5% by volume of concrete. Moreover, the enhanced post-cracking behaviour and crack control due to the presence of fibres can also potentially determine a significant increase in concrete shear

strength, thus leading to the possibility of partially or totally substituting conventional shear reinforcement [e.g., 9-14]. This last aspect could be particularly effective in order to lessen the congestion of reinforcement in the critical regions of RC framed structures, so leading to a more rational and efficient design, especially in seismic zones. In order to correctly take into account the effective contribution provided by steel fibres in the post-cracking structural response, the analysis of SFRC members should be carried out by using proper constitutive models, different from those currently adopted for ordinary reinforced concrete structures. To this scope, the 2D-PARC model, already developed for RC elements subjected to plane stresses [15-16], has been also extended to SFRC ones, by including a proper softening law [3] which takes into account the additional transmission of tensile stresses across cracks arising from the bridging effect of fibres.

2D-PARC MODEL FOR CRACKED SFR CONCRETE

The theoretical formulation of the adopted constitutive relation, which has been originally developed for ordinary RC elements, can be found in details in [15]. In this work, the main features of the model will be only briefly outlined, while the attention will be primarily focused on the evaluation of the resistant contribution offered by steel fibres in the composition of the material stiffness matrix.

Description of the model

The adopted model, which refers to a SFRC membrane element subjected to general plane stresses (Fig. 1), is based on a smeared-fixed crack approach.

In the uncracked stage, concrete and steel are treated like two materials working in parallel, by assuming perfect bond between them, while fibre contribution is neglected. Crack formation takes place when the maximum principal stress exceeds concrete tensile strength; furthermore, crack pattern is hypothesised as fully developed with a constant spacing a_{m1} (Fig. 1a).

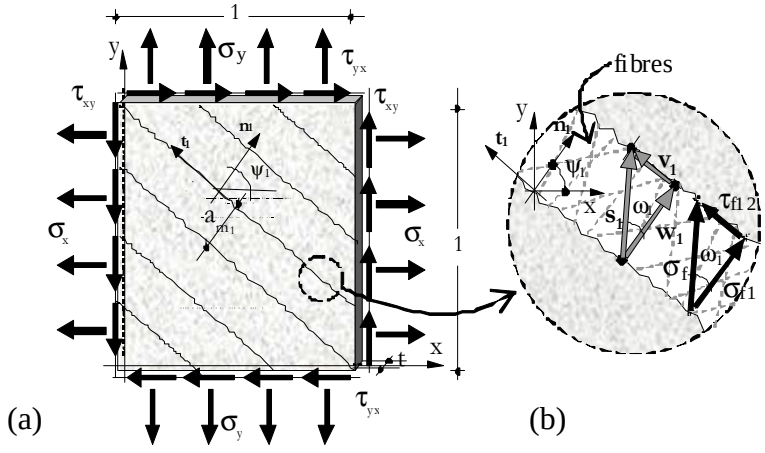

Figure 1. (a) SFRC membrane element in the cracked stage: geometry and notations; (b) kinematical parameters of the crack.

In the cracked stage, the model follows a strain decomposition procedure; as a consequence, the total strain $\{\varepsilon\}$ can be subdivided into two contributions, which are respectively represented by the strain $\{\varepsilon_c\}$ of SFRC between two adjacent cracks (still intact, even if damaged) and the one of the fracture zone $\{\varepsilon_{cr1}\}$, related to all the phenomena taking place at crack surfaces (Fig. 2). This last strain vector is first evaluated in the local coordinate system of the crack, n_1-t_1, as a function of the two reference kinematical variables showed in Fig. 1b, that are crack opening w_1 and sliding v_1, and subsequently transferred into the global coordinate system x-y.

Similarly to the uncracked stage, the stress field in SFRC between two adjacent cracks can be expressed as the sum of the stresses in the two materials, that are concrete and steel (Fig. 2), which can be evaluated as the product between the correspondent stiffness matrices, $[D_c]$ and $[D_s]$, and their strains, $\{\varepsilon_c\}$ and $\{\varepsilon_s\}$. The two matrices are simply derived from the corresponding ones calculated in the uncracked stage, by degrading their terms through a proper damage coefficient; as a consequence, the fibre contribution in the intact material between cracks is still neglected, and it is only explicitly considered in the evaluation of the crack stiffness sub-matrix $[D_{c,cr1}]$, as explained in the following. It should be also pointed out that in this stage the hypothesis of perfect bond is no longer valid, and consequently the two strain vectors, $\{\varepsilon_c\}$ and $\{\varepsilon_s\}$, cannot be assumed coincident with each other. Anyway, for the sake of simplicity, the steel strain $\{\varepsilon_s\}$ has been assumed coincident with the total average strain $\{\varepsilon\}$, due to the limited difference between them.

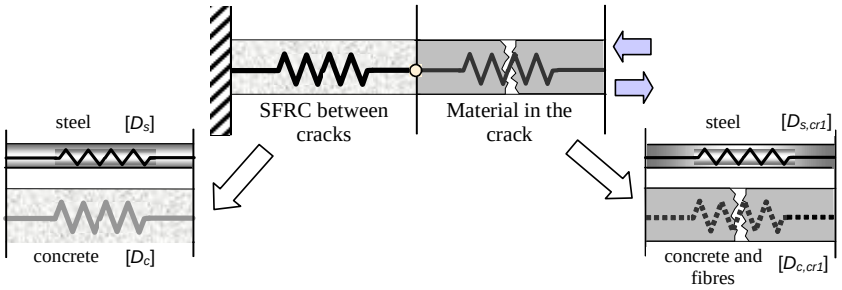

Figure 2. Sketch of the uncracked SFRC and of the crack as "materials" in series.

As regards the stress field in the crack, it can be determined once again as the product between the crack stiffness matrix, $[D_{cr1}]$, and the strain vector of the fracture zone, $\{\varepsilon_{cr1}\}$, having assumed that:

$$[D_{cr1}] = [D_{c,cr1}] + [D_{s,cr1}] \tag{1}$$

by separately considering the contributions related to SFR concrete and ordinary steel bars crossing the cracks. The first one accounts for aggregate bridging and interlock, as well as for fibre bridging and prestress, and can be expressed in the local coordinate system of the crack in the following form:

$$\left[\; D_{c,cr1}^{(n_1,t_1)} \; \right] = \begin{bmatrix} c_{b1} + c_{f1} & -c_{01} \\ 0 & c_{a1} + c_{f1} \end{bmatrix}. \tag{2}$$

The resistant mechanisms associated with aggregates and fibres are evaluated independently, following a micro-mechanical approach originally proposed by Li et al. [3]. More in details, the aggregate bridging action is expressed as a function of crack opening w_1, through an empirical relation (reported in [15]) calibrated on the basis of several experimental data, and it is taken into account through the bridging coefficient c_{b1}. Fibre action is instead represented through the coefficient c_{f1}, which is derived from the following relations:

$$\sigma_{f1}(s_1) = \sigma_f(s_1)\ \cos\omega_1 = \sigma_f(s_1)\ \frac{w_1}{\sqrt{{w_1}^2 + {v_1}^2}} = c_{f1}\ \varepsilon_1 \tag{3}$$

$$\tau_{f12}(s_1) = \sigma_f(s_1)\ \sin\omega_1 = \sigma_f(s_1)\ \frac{v_1}{\sqrt{{w_1}^2 + {v_1}^2}} = c_{f1}\ \gamma_{12} \tag{4}$$

being $\varepsilon_1 = w_1/am_1$ and $\gamma_{12} = v_1/am_1$, while σ_{f1} and τ_{f12} are the normal and tangential components of the total fibre contribution σ_f, according to Fig. 1b, which is in turn calculated by adding the bridging effect developed by the fibres themselves in the fracture region, σ_b, and the fibre prestress that is present before crack formation, σ^0_{ps}:

$$\sigma_f(s_1) = \sigma_b(s_1) + \sigma^0_{ps}(s_1)\,. \tag{5}$$

As can be seen, all these terms have been expressed as a function of the total displacement across the crack, s_1, representing the resultant of crack opening w_1 and sliding v_1, according to Fig. 2b. On concrete side, the stiffness matrix $[D_{c,cr1}]$ (reported in Eq. 2) also includes the aggregate interlock effect, evaluated according [17], through the coefficients c_{a1} and c_{01}, whose expression can be found in [15].

As regards the sub-matrix $[D_{s,cr1}]$, related to the resistant mechanisms due to steel bars crossing the crack (that is tension stiffening and dowel action, see Eq. 1 and Fig. 2), it can be obtained by summing up the contribution of each *i-th* reinforcement layer:

$$\left[\ D^{(x_i,y_i)}_{si,cr1}\ \right] = \rho_{si} \begin{bmatrix} \overline{E}^{cr1}_{si}\ g_{i1} & 0 \\ 0 & d_{i1} \end{bmatrix}, \tag{6}$$

which is first evaluated in its local coordinate system x_i-y_i, according to [15], and then transposed into the global one. Finally, the global stiffness matrix of the SFRC cracked element can be obtained from previous equations, by simply deducing the two strain vectors $\{\varepsilon_c\}$ and $\{\varepsilon_{cr1}\}$ from the two equilibrium conditions (respectively relative to the intact material between cracks and to the fracture zone), and substituting their values into the compatibility equation, as reported in [15].

Implementation of the model into a FE procedure

The above described stiffness matrices have been implemented into a commercial FE code (ABAQUS [18]) in the form of a "user-material" subroutine, in order to perform

numerical analyses on different SFRC structural elements, able to account for both material non-linearity and fibre resistant contribution in the post-cracking stage.

At each loading increment (or iteration within a fixed increment) and for each single element in which the structure is subdivided, the total strain vector $\{\varepsilon\}$ calculated from the adopted FE code is passed to the user-material subroutine. Following the above described procedure, these strain values are used for the evaluation of the proper material stiffness matrix depending on the current cracking stage and, known it, for the determination of corresponding stresses, which are then passed back to the FE code for the execution of external convergence checks. On this point, it should be reminded that the proposed model is based on a strain decomposition scheme in the cracked stage; as a consequence, it is also necessary to check the convergence on total strain through an internal iterative procedure, like the one summarized in the flow chart reported Fig. 3.

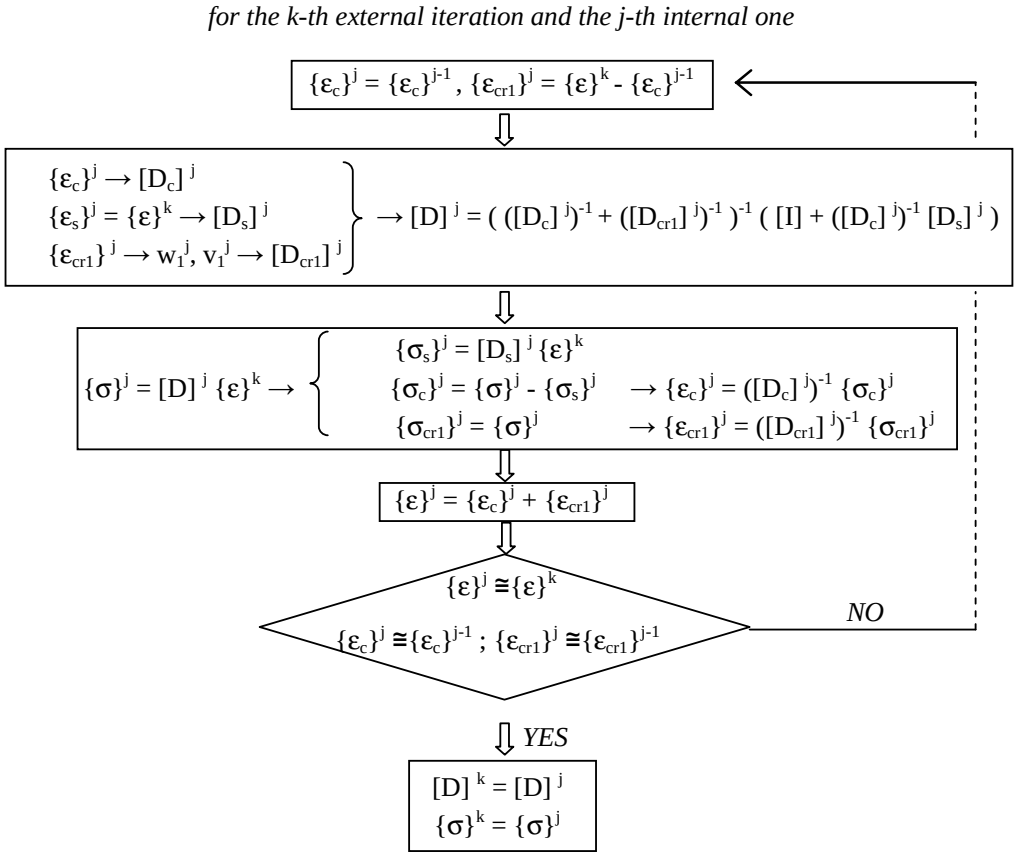

Figure 3. Flow chart of the internal iterative procedure to obtain strain decomposition.

COMPARISONS WITH EXPERIMENTAL RESULTS

SFRC beams in bending

In order to verify the effectiveness of the proposed procedure, an experimental program carried out on SFRC beams in bending has been first considered [8]. More in details,

four point bending tests have been performed on three identical specimens, produced with a C20/25 concrete and DRAMIX-RC-80/0.60-BN fibres, characterised by a length of 60 mm, a diameter equal to 0.75 mm, and a fibre dosage equal to 30 kg/m^3. The specimens were under-reinforced, since the provided reinforcement ratio ρ has been kept equal to 0.00315. In addition, a transversal reinforcement constituted by 8 mm stirrups, with 100 mm spacing, has been included in the beams. More details about reinforcement distribution and material properties can be found in [8] and are partly summarised in Fig. 4, where also geometrical details of the test are indicated.

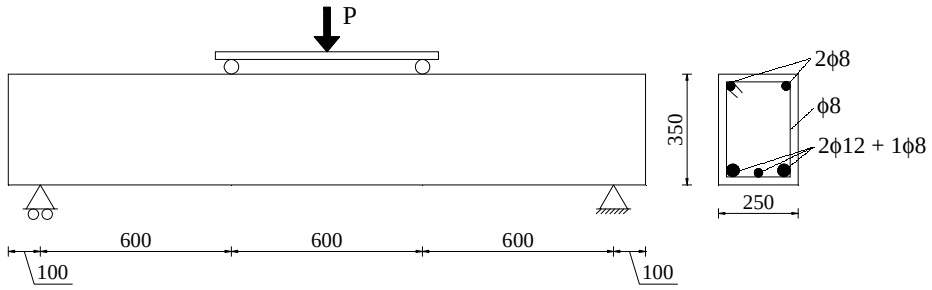

Figure 4. Sketch of the loading arrangement adopted during the experimental test and beam cross-section details [8] (dimensions in mm).

Taking advantage of the symmetry of the problem, only one half of the SFRC beam has been modelled, by adopting a FE mesh constituted by quadratic, isoparametric 8-node membrane elements with reduced integration (4 Gauss integration points).

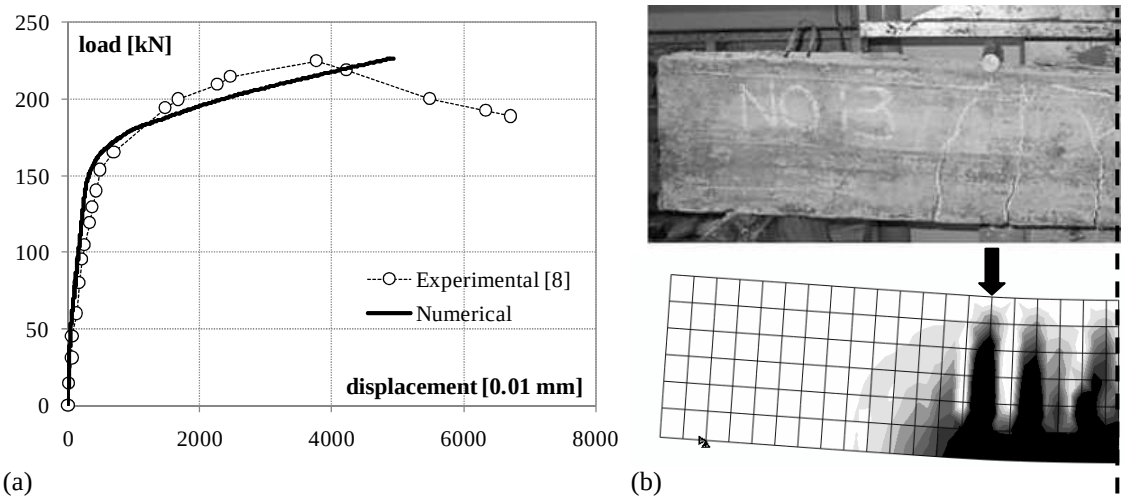

Figure 5. Comparisons between numerical and experimental [8] results, in terms of: (a) applied load vs. deflection at midspan; (b) crack pattern at failure.

The main comparisons between experimental and numerical results have been provided in terms of load-deflection response, as well as crack pattern at failure, and are summarised in Fig. 5. As can be observed, the adopted procedure is able to correctly predict the experimental failure load, even if the maximum achieved deflection at midspan is slightly underestimated. As regards the crack pattern at failure, both the

experimental and numerical responses are mainly interested by the appearance of vertical flexural cracks in the central part of the SFRC beam, which are characterised by an increasing extension, as well as by greater crack widths as the applied load increases.

SFRC beams in shear

The attention has been then focused on three SFRC beams without ordinary transversal reinforcement and subjected to shear, which are part of a more extensive experimental program recently carried out at the University of Brescia [14].

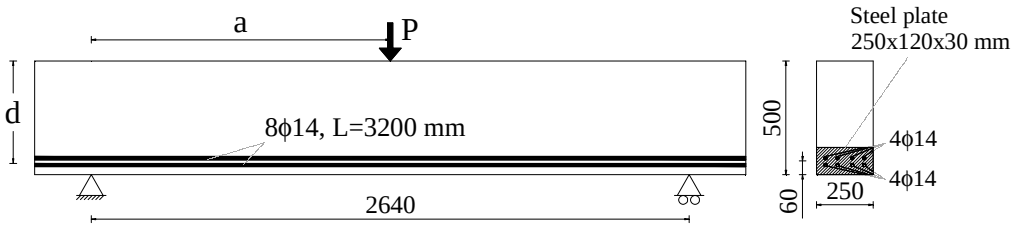

Figure 6. Sketch of the loading arrangement adopted during the experimental test and beam cross-section details [14] (dimensions in mm).

The considered specimens are characterised by the same geometry (reported in Fig. 6) and by the same longitudinal steel ratio ρ, which has been set almost equal to 0.01, while a different amount of steel fibres has been added to the concrete mix. More in details, steel fibre dosage has been respectively set equal to 0 (plain concrete "reference" specimen), 50 and 75 kg/m^3, while the type of reinforcement has been kept the same, that is to say hooked end fibres, with a length of 50 mm, a diameter of 0.8 mm and a tensile strength equal to 1100 MPa. A normal strength concrete (f_{ck} of about 30 MPa) has been used for beam casting. The three considered beams have been tested under a three point loading system, providing a shear span-to-depth ratio a/d almost equal to 3, as indicated in Fig. 6. Further details about specimen configuration, material properties and test arrangement can be found in [14].

Also in this case, the FE mesh has been realised by following the same criteria already described for the simulation of the bending test. The main comparisons between experimental and numerical results have been again provided in terms of applied load vs. deflection under the loading point and are reported in Figs. 7a-c. As can be observed, the proposed model is able to correctly model the enhanced post-cracking behaviour of SFRC specimens with respect to the reference one made of plain concrete (indicated as PC), since the corresponding curves are not only characterised by an higher peak load, but also by a different failure mode, which passes from shear to flexure, with a clear yielding of the longitudinal reinforcement and a rather significant ductility especially for specimen FRC50 (with 50 kg/m^3 of fibres). Figure 7d also shows the numerical crack pattern at failure for specimens PC and FRC50; as can be seen, the addition of fibres determines a stable propagation and progressive development of several cracks with a reduced spacing, so leading to a more ductile behaviour, with the development of vertical deflections that are significantly greater than those obtained for the reference plain concrete specimen. This latter is instead characterised by the spreading of a main shear crack, which is immediately followed by element failure.

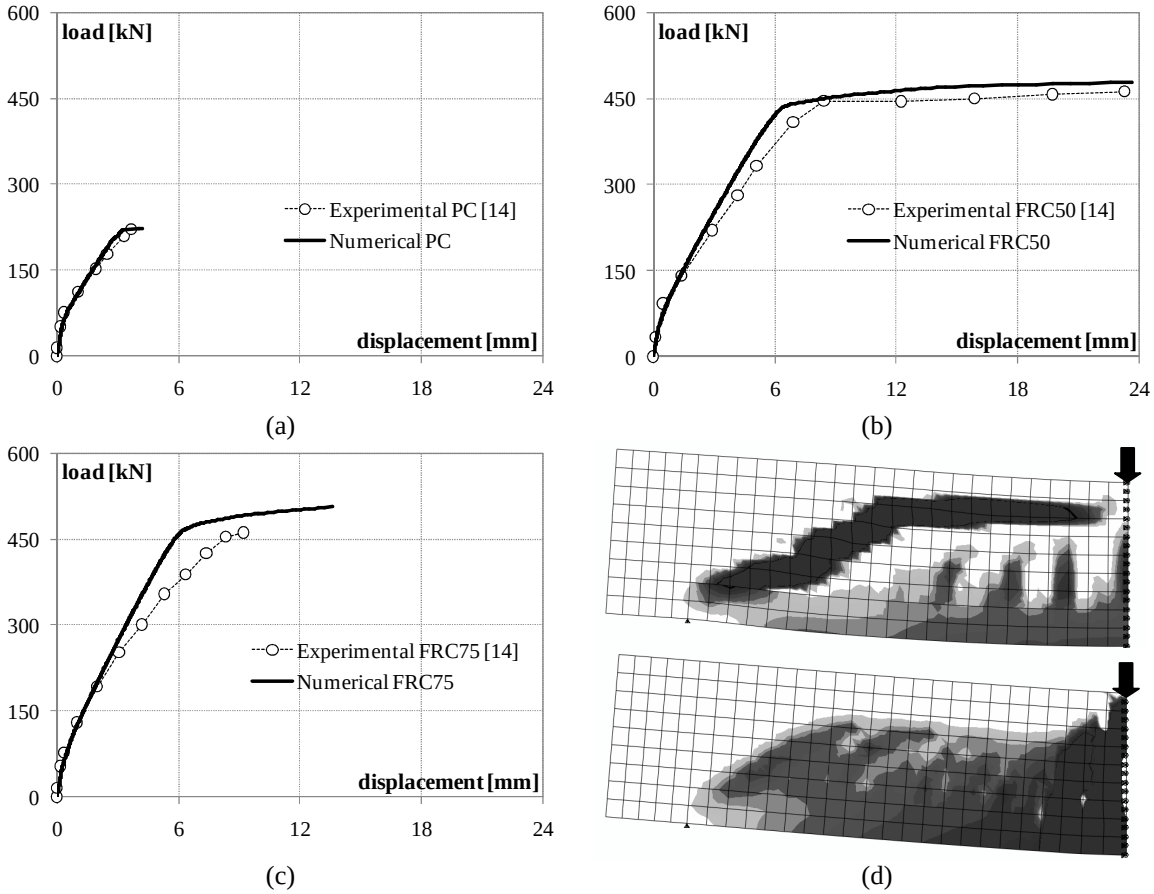

Figure 7. Comparisons between numerical and experimental [14] results, in terms of applied load vs. deflection at midspan for: (a) plain concrete specimen PC and for SFRC specimens with (b) 50 kg/m^3 (FRC50) and (c) 75 kg/m^3 (FRC75) amount of fibres; (d) numerical crack pattern at failure for PC (above) and FRC50 (below) specimens.

CONCLUSIONS

In this work, an extension of 2D-PARC constitutive model to SFRC elements subjected to plane stresses is presented, by including a realistic constitutive law [3] able to account for fibre contribution in the post-cracking stage. After its implementation into a FE code, the proposed model has been applied to the analysis of SFRC beams subjected to bending and shear, and its effectiveness has been proved through comparisons with some experimental results available in technical literature [8,14]. The good agreement between numerical provision and physical reality confirms the need to adopt more complex models - like the one presented, based on fracture mechanics concepts - in the design of these structural elements. Further validations of the proposed approach will also concern SFRC shear critical beams with and without stirrups, in order to investigate the effective possibility of using steel fibres as minimum shear reinforcement.

REFERENCES

1. Shah, S.P., Rangan, B.V. (1971) *ACI J. Proc*. **68**(2), 126-137.
2. Barros, J.A.O., Figueiras, J.A. (1999) *ASCE J. Mat. Civ. Eng.* **11**(4), 331-339.
3. Li, V., Stang, H., Krenchel, H. (1993) *Mat. Struct*. **26**, 486-494.
4. Furlan, JrS., de Hanai, J.B. (1997) *Cem. Concr. Compos.* **19**(4), 359-366.
5. Swamy, R.N., Al-Ta'an, S.A. (1981) *ACI Struct. J.* **78**(3), 395-405.
6. Dupont, D., Vandewalle, L. (2002). In: *Proc. Int. Congress on Challenges of Concr. Constr.*, Dundee, 81-90.
7. Campione, G., Mangiavillano, M.L. (2008) *Eng. Struct* **30**, 2970-2980.
8. Őzcan, D.M., Bayraktar, A., Sahin, A., Haktanir, T., Tűrker, T. (2009) *Constr. Build. Mat.* **23**, 1064-1077.
9. Lim, D.H., Oh, B.H. (1999) *Engng. Struct.* **21**, 937-944.
10. Cucchiara, C., La Mendola, L., Papia, M. (2004) *Cem. Concr. Res.* **26**, 777-786.
11. Susetyo, J., Gauvreau, P., Vecchio, F.J. (2011) *ACI Struct J.* **108**(4), 488-496.
12. Dinh, H.H., Parra-Montesinos, G.J., Wight, J.K. (2010) *ACI Struct. J.* **107**(5), 597-606.
13. Minelli, F., Plizzari, G.A. (2008). In: *Proc. fib Symposium "Tailor Made Concr. Struct.-New solutions of our Society"*, 605-610.
14. Minelli, F., Plizzari, G.A. (2010). In: *fib Bulletin 57 - Shear and punching shear in RC and FRC elements*, 211-225.
15. Cerioni, R., Iori, I., Michelini, E., Bernardi, P. (2008) *Eng. Frac. Mech*. **75**(3-4), 615-628.
16. Cerioni, R., Bernardi, P., Michelini, E., Mordini, A. (2011) *Eng. Frac. Mech*. **78**, 1784-1793.
17. Gambarova, P.G. (1983). In: *Proc. AICAP Conference*, Bari, 141-156.
18. Abaqus 6.10 (2010) *Online documentation*, Dassault Systémes Simulia Corp.